



Calix[4]pyrroles: Versatile molecular containers with ion transport, recognition, and molecular switching functions

| | |
|-------------------------------|--|
| Journal: | <i>Chemical Society Reviews</i> |
| Manuscript ID: | CS-REV-05-2014-000157.R1 |
| Article Type: | Review Article |
| Date Submitted by the Author: | 07-May-2014 |
| Complete List of Authors: | Kim, Dong Sub; The University of Texas at Austin, Chemistry Sessler, Jonathan; The University of Texas at Austin, Chemistry |
| | |

ARTICLE

Calix[4]pyrroles: Versatile molecular containers with ion transport, recognition, and molecular switching functions

Cite this: DOI: 10.1039/x0xx00000x

Dong Sub Kim and Jonathan L. Sessler

Received 00th January 2012,
Accepted 00th January 2012

DOI: 10.1039/x0xx00000x

www.rsc.org/

Over the last two decades, calix[4]pyrroles have attracted considerable attention as molecular containers. Used in this capacity, they have been exploited as strong and selective receptors and as extractants for both anions and ion pairs. More recently, calix[4]pyrroles have found application as carriers, systems capable of transporting ions and ion pairs across lipophilic membrane. The use of calix[4]pyrroles as building blocks for the preparation of stimulus-responsive material has also been demonstrated. In this latter context, as well as others, the conformational switching, from 1,3-alternate to cone upon anion binding has been exploited to control both structure and substrate binding. In this Review, we describe recent results involving the use of calix[4]pyrrole systems for ion transport. Also summarised is work devoted to the formation of higher order supramolecular aggregates and studies of their response to external stimuli. Taken together, these examples serve to highlight new uses of calix[4]pyrroles as molecular containers.

Introduction

A container, in general, is an object used for, or capable of, holding liquids, gases, or one or more other solid objects. In common parlance, containers are recognized as being especially useful for transport or storage. Macroscopic containers are frequently used to sort or separate objects of interest from other species such that the separated object may be more readily identified, stored, or accessed. On a molecular scale, so-called 'molecular containers' play similar roles. However, they typically exploit molecular recognition strategies involving a variety of secondary interactions, such as H-bonds, metal-ligand, hydrophobic interactions, and the like. In recent years, considerable effort has been devoted to the development of artificial molecular entities that can function as container-like systems. The interest in such systems is driven in part by their potential utility in areas as diverse as catalysis, recognition, separation, and transport. In this Review, we illustrate the use of calix[4]pyrrole-based systems as ion transporters and as building blocks for molecular self-assembly. In so doing, we have tried to highlight two applications of these venerable systems as molecular containers.

Calix[4]pyrrole (**1**) was first reported in the 19th century.¹ As a class, calix[4]pyrroles have been extensively examined as anion receptors for the last two decades and it is now appreciated that these non-aromatic tetrapyrroles bind a variety of anions

including, halides, acetates, phosphates in aprotic media.²⁻⁴ More recently, potential applications of calix[4]pyrroles as carriers, species capable of transporting ions across lipophilic membranes, have been reported.⁵⁻¹⁰ In addition to being relatively easy to synthesise, the ditopic nature of calix[4]pyrrole derivatives allows them to act as receptors and extractants for both anions and cations under appropriately chosen conditions. In particular, complexation of an anion to calix[4]pyrrole *via* four hydrogen bonds drives conversion from the 1,3-alternate to the cone conformation. This conversion provides a concave, bowl-like cavity that permits recognition of charge diffuse cations, such as caesium and imidazolium, through cation – π interactions.¹¹ Functionalisation of the calix[4]pyrrole *meso* or β -pyrrolic positions allows the incorporation of additional binding sites for cations. Recently, the conversion between the 1,3-alternate and cone conformations has been exploited to create self-assembled molecular ensembles that respond well to external stimuli.¹²⁻¹⁴ It is this combination of features, namely ion transport capability and chemical stimulus controlled self-assembly, that makes calix[4]pyrroles of particular interest as molecular containers.

Transport of chloride and other anions: Calix[4]pyrrole-based molecular carriers

Biological ion channels play important roles in a large number of cellular functions, including control and modulation of transmembrane potentials, chemical signaling, transepithelial ion transport, regulation of cytoplasmic or vesicular ion concentrations, pH control, and regulation of cell volume.¹⁵ Malfunction of ion channel function is correlated with a variety of disorders, such as cystic fibrosis, Bartter's syndrome, Dent's disease, myotonia, epilepsy,^{15,16} and can result in kidney failure, reduced bone strength, cardiac stress, and nerve system problems. Not surprisingly, therefore, considerable attention has been devoted to the development of synthetic compounds that are capable of facilitating ion transport across lipid bilayer membranes. Such systems may help shed light on biological transport processes and, ultimately, may offer a pharmacological solution to medical disorders involving misregulated biological ion transport. Over the last two decades, considerable progress has been made in the field and there are now a number of synthetic ion transporters and channel mimics known. As yet, however, no synthetic ion transport system has entered clinical development and our understanding of the basic mechanisms of transport remains in its infancy. The design principles that will give rise to synthetic ion transporters (or channels) capable of functioning in complex biological environment are likewise far from understood. In this section we summarise the use calix[4]pyrroles as carriers for the through-membrane transport of anions and ion pairs.

Octamethylcalix[4]pyrrole: A simple yet effective chloride anion transporter that can operate *via* different transport mechanisms

The first evidence that calix[4]pyrrole (**1**) could function as a potential ion carrier across lipid bilayer membrane came from



Mr. Dong Sub Kim obtained his BS degree (*magna cum laude*) in chemistry in 2006 and MS degree in organic chemistry in 2008 from Sogang University in Seoul, Korea under the supervision of Professor Won Koo Lee. After serving as a research associate at the Korea Institute of Science and Technology (KIST) under the

guidance of Dr. Hyunjoo Lee and Professor Hoon Sik Kim, he joined the Sessler group at The University of Texas at Austin in 2009 to pursue his PhD. His research focuses on the development of calix[4]pyrrole-based stimuli-responsive materials and molecular self-assembly.

the Quesada, Sessler, and Gale groups in 2008.⁹

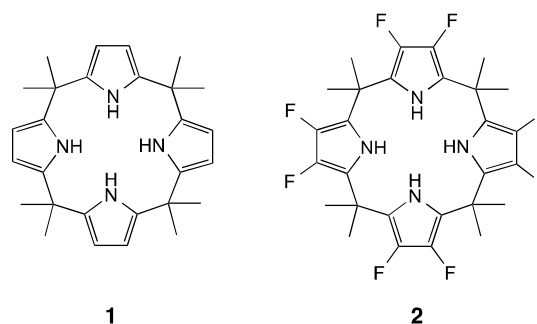


Fig. 1 Chemical structures of octamethylcalix[4]pyrrole **1** and octafluorocalix[4]pyrrole **2**.

These researchers studied the parent calix[4]pyrrole **1** as a possible carrier for simple salts using 1-palmitoyl-2-oleyl-sn-glycero-3-phosphocholine (POPC) vesicles as a membrane mimic. In this study, the POPC vesicles were loaded with CsCl and suspended in two different external solutions; one contained NaNO₃, whereas the other contained Na₂SO₄. The sulphate ion is highly hydrophilic.¹⁷ It was not expected to be soluble in the lipophilic membranes or to pass through the membrane at an appreciable rate. On the other hand, the nitrate anion is sufficiently hydrophobic that it was expected to allow anion/nitrate exchange. This exchange is required for charge neutralisation under so-called antiport ion transport scenarios. It would not be required when the calix[4]pyrrole serves to co-transport both an anion and a counter cation. These limiting mechanisms are discussed further below and illustrated schematically in Figures 2 and 3.



Prof. Jonathan L. Sessler received a BS degree (with Highest Honours) in chemistry in 1977 from the University of California, Berkeley and a PhD in organic chemistry from Stanford University in 1982 (supervisor: Professor James P. Collman). After completing NSF-CNRS and NSF-NATO Postdoctoral Fellowships with Professor Jean-Marie Lehn at L'Université Louis Pasteur de Strasbourg, France, he was a JSPS Visiting Scientist in Professor Tabushi's group in Kyoto, Japan. In September 1984, he accepted a position as an Assistant Professor of Chemistry at the University of Texas at Austin, where he is currently the Roland K. Pettit Chair. To date, Dr Sessler has authored 600 research publications, written two books, and been an inventor of record on almost 80 issued U.S. Patents. Dr Sessler is a co-founder of

Pharmacycelics, Inc., a publicly traded company (peyc;

In these first studies, calix[4]pyrrole **1** as a DMSO solution was added to the vesicular suspension at 2% of the lipid concentration. Chloride anion efflux was then monitored using a chloride selective electrode. The vesicles were lysed using detergent after five minutes, and the final reading of the electrode was set to 100% release of chloride. Under these conditions, octamethylcalix[4]pyrrole **1** proved to be an effective ion carrier over the course of the five minute experimental window. This was found to hold true both for vesicles suspended in external solutions containing either the sulphate or nitrate anions. In a separate experiment designed to probe the cation dependent nature of the transport process, it was found that chloride efflux was seen in the case of vesicles loaded with caesium chloride, but not those containing NaCl, KCl, or RbCl. These findings led to the conclusion that this particular calix[4]pyrrole acts as a selective co-transporter of CsCl, as shown schematically in Fig. 2. This limiting mechanism is also referred to as “symport”.

Interestingly, the β -octafluoro-substituted analogue of the parent macrocycle (i.e., **2**) was found to function as an anion carrier *via* a chloride/nitrate antiport mechanism.⁹ Support for this proposed mechanism came from the finding that the transport rate was essentially independent of the choice of inner cation. Specifically, and in contradistinction to what was seen in the case of the parent octamethylcalix[4]pyrrole **1**, chloride efflux was observed in all vesicles studied, including those containing NaCl, KCl, and RbCl provided the external solution contained NaNO₃ rather than Na₂SO₄. This lack of cation dependence on the rate of chloride transport across the POPC membrane is consistent with the suggestion that calix[4]pyrrole **2** facilitates chloride transport *via* an antiport mechanism, namely exchange of chloride for nitrate as shown schematically in Fig. 3. Further support for the proposed antiport mechanism came from studies where Na₂SO₄ was used in lieu of NaNO₃ in the external solution. Under these conditions, the octafluoro-substituted calix[4]pyrrole **2** does not act as an effective chloride anion carrier. This inversion in transport mechanism from co-transport to antiport on going from **1** to **2** was rationalized in terms of the octafluoro derivative **2** having a higher affinity for the chloride anion, yet a lower affinity towards various accompanying counter cations, including Cs⁺, than the original system **1**.

Carrier **2** was also found to facilitate chloride/bicarbonate antiport. This conclusion is based on the finding that vesicles loaded with NaCl and suspended in a solution of Na₂SO₄ demonstrate little appreciable chloride efflux. However, when after 120 s, NaHCO₃ is added to the system chloride transfer from within the vesicles to the outer receiving phase was observed. The same experiment was preformed with compound **1**. However, no evidence of significant chloride transport was seen.

Modulating chloride transport *via* strapped calix[4]pyrroles

NASDAQ) dedicated to developing new cancer therapies.

Over the last two decades, considerable effort has been devoted to the creation of chemosensors for anionic species that are based on the use of a calix[4]pyrrole scaffold. The most widely used approaches to creating such sensors involves functionalisation of either the pyrrolic β -positions or *meso* positions. An offshoot of these generalized efforts was the development of so-called “strapped” calix[4]pyrroles by the Lee and Sessler groups.^{18,19} Depending on the nature of the straps, these *meso*-functionalised calix[4]pyrroles can display higher anion binding affinities or recognise anions or ion pairs with greater selectivity than their unstrapped analogues.¹⁹⁻²² These particular container systems are also appealing as ion carriers. However, to date, only a few strapped calix[4]pyrroles have been studied in this regard.

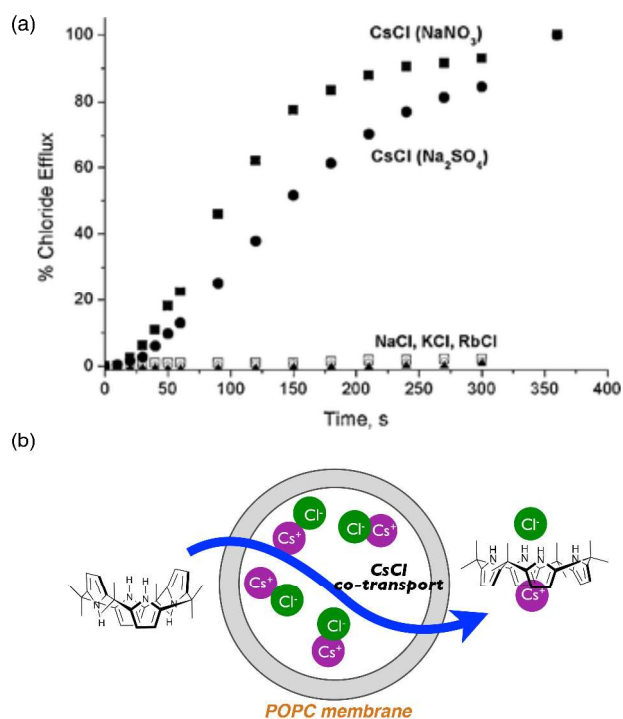


Fig. 2 (a) Chloride efflux promoted upon addition of **1** (2 mole % carrier to lipid) to unilamellar POPC vesicles loaded with 488 mM CsCl (■), RbCl (○), KCl (▲), or NaCl (□), as well as 5 mM phosphate buffer, pH 7.2, dispersed in 488 mM NaNO₃, 5 mM phosphate buffer, pH 7.2, and unilamellar POPC vesicles loaded with 488 mM CsCl (●), 5 mM phosphate buffer, pH 7.2, dispersed in 162 mM Na₂SO₄. (b) Schematic representation of CsCl co-transport mediated by **1**.

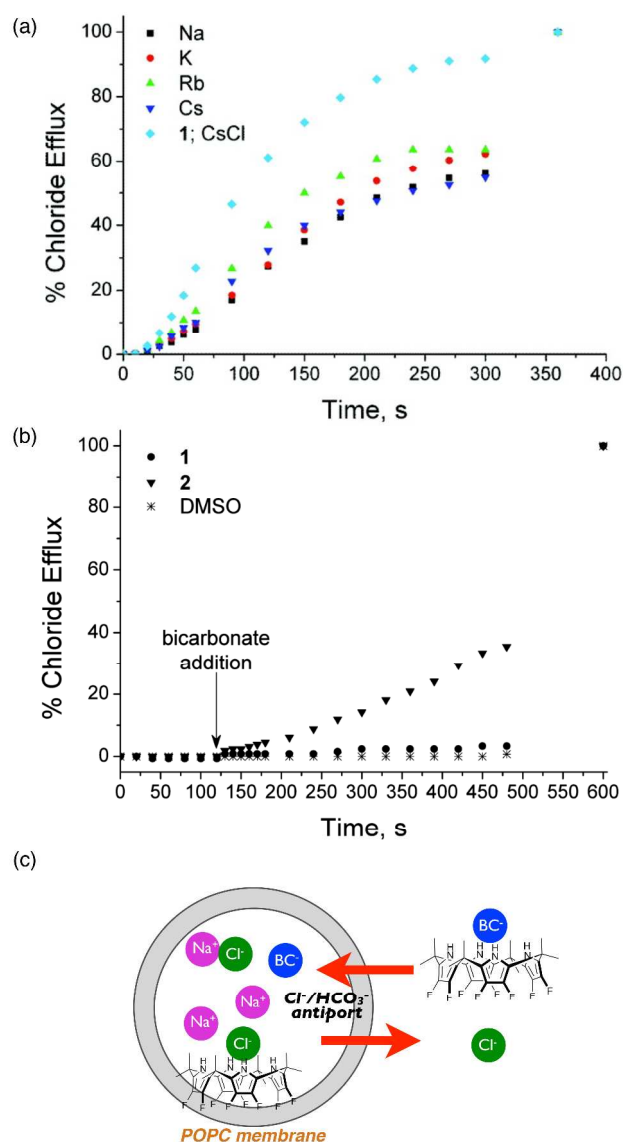


Fig. 3 (a) Chloride anion efflux promoted by **2** across POPC vesicles loaded with sodium, potassium, rubidium, and caesium chloride salts buffered at pH 7.2 with 5 mM phosphate. Also shown and specifically denoted in the figure inset is a comparison experiment involving chloride anion efflux promoted by **1** across POPC vesicles loaded with caesium chloride. The vesicles were dispersed in Na₂SO₄ buffered at pH 7.2 with 5 mM phosphate. (b) Chloride efflux promoted by **1** and **2** across POPC vesicles loaded with NaCl buffered at pH 7.2 with 20 mM phosphate upon addition of a NaHCO₃ pulse. (c) Schematic representation of Cl⁻/HCO₃⁻ antiport mediated by **2**. (BC⁻ = bicarbonate) Adapted with permission from *J. Am. Chem. Soc.*, 2010, **132**, 3240-3241. Copyright 2010 American Chemical Society.

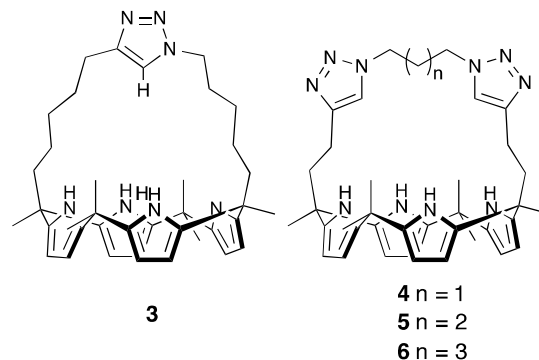


Fig. 4 Chemical structures of 1,2,3-triazole-strapped calix[4]pyrroles **3-6**.

In 2009, Gale and coworkers synthesised a 1,2,3-triazole-strapped calix[4]pyrrole (**3**) and demonstrated its ability to transport chloride anions across lipid bilayer membranes.⁷ Slow exchange kinetics were revealed for the interaction between **3** and chloride anions on the ¹H NMR time scale. Therefore, the chloride anion affinities were evaluated by isothermal titration calorimetry (ITC) in acetonitrile solution using tetraethylammonium chloride (TEACl) as the chloride anion source. On the basis of this analysis, it was concluded that the strapped system **3** binds the chloride anion about an order of magnitude more effectively than the parent calix[4]pyrrole **1**. Most of this increase is enthalpic in origin (cf. Table 1).

Table 1 Energetics of tetraethylammonium chloride binding to calix[4]pyrroles **1** and **3** in acetonitrile solution at 303 K as determined by ITC

| Host | $K_{\text{ass}} / \text{M}^{-1}$ | $\Delta G^\circ / \text{kcal mol}^{-1}$ | $\Delta H^\circ / \text{kcal mol}^{-1}$ | $T\Delta S^\circ / \text{kcal mol}^{-1}$ |
|----------|----------------------------------|---|---|--|
| 1 | 1.9×10^5 | -7.19 | -10.1 | -3.07 |
| 3 | 1.3×10^6 | -8.47 | -12.0 | -3.52 |

To elucidate the transport mechanism, Gale and coworkers carried out experiments analogous to those described above. Specifically, POPC vesicles loaded with CsCl, RbCl, KCl or NaCl were suspended in external buffered solution containing NaNO₃. Unlike the parent system **1**, with the triazole-strapped calix[4]pyrrole **3**, chloride anion transport was seen in the case of all four sets of vesicles. As would be expected for a cation-anion co-transport mechanism, the most effective transport was seen in the case of the vesicles containing the relatively more hydrophobic caesium cation.

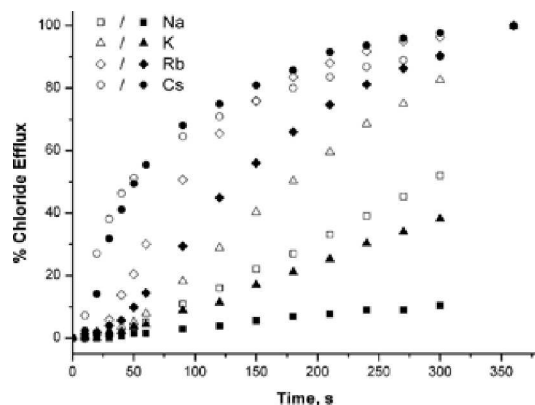


Fig. 5 Chloride efflux promoted by **3** across POPC vesicles loaded with NaCl, KCl, RbCl or CsCl buffered to pH 7.2 with 5 mM phosphate dispersed in NaNO₃ (open symbols) or Na₂SO₄ (closed symbols). Originally published in *Chem. Commun.*, 2009, 3017-3019. Copyright Royal Society of Chemistry.

To analyse further the mechanism of transport operative in the case of compound **3**, similar experiments were carried out with Na₂SO₄ in the external phase (Fig. 5). In contrast to the parent calix[4]pyrrole **1**, the 1,2,3-triazole-strapped macrocycle **3** proved capable of transporting chloride anions across the membrane under these conditions. However, in the case of the vesicles containing potassium and sodium chloride, a substantial drop in the rate of chloride release was seen when the external solution was changed from NaNO₃ to Na₂SO₄. In contrast, for the vesicles containing caesium chloride, little dependence on the choice of external anion (nitrate vs. sulphate) was seen. This disparity was rationalised in terms of the predominant chloride transport mechanism being influenced by the choice of counter cation: The large caesium cation allows for ion pair (Cs⁺ + Cl⁻) symport, while smaller and more hydrophilic cations, such as potassium and sodium, support chloride efflux only under conditions where a chloride/nitrate antiport transport mode is possible.

Insights into the relationship between the nature of the strap and the transport efficiency came from a vesicle transport study wherein the *bis*-triazole-strapped calix[4]pyrroles **4-6** were used as putative through membrane chloride anion carriers (Fig. 4).⁶ It was found that the more open calix[4]pyrrole container **6** promoted faster chloride efflux regardless of the Group I metal counter cation. This difference in transport efficiency was ascribed to multiple factors, including improved partitioning of the carrier into the lipid bilayer from the aqueous solution, higher mobility of the carrier within the membrane, and an improved solubilisation of the carrier-anion complex in the hydrophobic membrane.²⁰ Two X-ray crystal structures, specifically of the chloride-bound complexes of **5** and **6**, provided further support for this rationalization (Fig. 6). In the case of [5•Cl]⁻, the bound chloride anion is stabilised by five hydrogen bonds, including one from a triazole CH proton. On the other hand, compound **6** stabilises chloride anion complexation by providing six hydrogen bonds – four from the

calix[4]pyrrole NH protons and two from the triazole CH protons. The net result is that the chloride anion is more tightly bound. This has the further consequence that, presumably, the complex as a whole is less subject to energetically unfavourable desolvation effects upon moving into the more hydrophobic membrane phase.

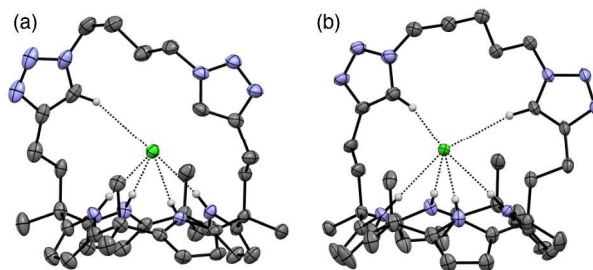


Fig. 6 Views of the single crystal X-ray diffraction structures of (a) [5•Cl]⁻ and (b) [6•Cl]⁻ complexes. Non-hydrogen-bonded H atoms, methanol solvent molecules, and the tetrabutylammonium (TBA⁺) counteranions are omitted for clarity.

While little dependence on the choice of external anion (nitrate vs. sulphate) was seen in the case of compound **4**, for compounds **5** and **6**, higher rates of chloride efflux were seen for the CsCl-containing vesicles suspended in NaNO₃ than for those with Na₂SO₄ in the outer phase (Fig. 7). These findings were interpreted in terms of the dominant transport mechanism changing from caesium/chloride co-transport to chloride/nitrate antiport upon moving from **4** to **5** and **6**.

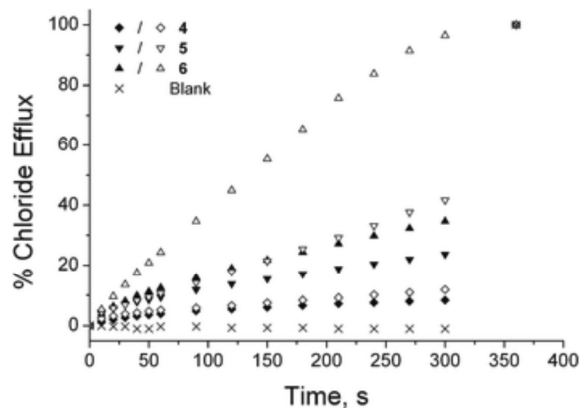


Fig. 7 Chloride efflux promoted by **4-6** in POPC vesicles loaded with CsCl salt. The vesicles were dispersed in Na₂SO₄ (closed symbols) or NaNO₃ (open symbols) with the carrier added as a DMSO solution. DMSO was used as a blank, negative control (x). Originally published in *Org. Biomol. Chem.*, 2010, **8**, 4356-4363. Copyright Royal Society of Chemistry.

Carriers and channels responsible for ion transport through biological membranes are typically highly dependent on the

nature of the cation. It was considered likely, therefore, that modulation of the counter cation binding features could also play an important role in modulating the transport capability of calix[4]pyrrole carriers. To test this hypothesis, Sessler, Gale Lee, and coworkers studied the oligoether-strapped calix[4]pyrrole ion pair receptor **7** (Fig. 8). This system has one anion binding site and two possible cation binding sites.²

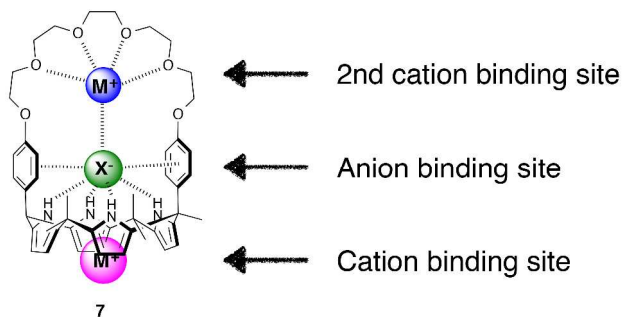


Fig. 8 Chemical structure of the oligoether-strapped calix[4]pyrrole **7**. Also shown are the putative anion and cation binding sites.

The binding properties of this hybrid calix[4]pyrrole receptor are dependent on the choice of Group I metal counter cations. For example, ¹H NMR spectroscopic studies revealed that the addition of potassium and caesium cations (as the perchlorate salts) to 10% CD₃OD/CD₃CN solutions of the preformed TBA⁺[**7**•F]⁻ complex gives rise to two distinct ion pair complexes (Fig. 9). In the case of K⁺, the cation is bound within the oligoether strap. In contrast, the caesium cation is bound to the cup-like cavity of the calix[4]pyrrole. In the case of the caesium-containing complex, a downfield shift was seen for the β-pyrrolic protons with no discernable changes in the oligoether strap signals being observed; this is consistent with the conclusion that the caesium cation is bound within the ‘cup’ of the calixpyrrole container as shown schematically in Fig. 9.

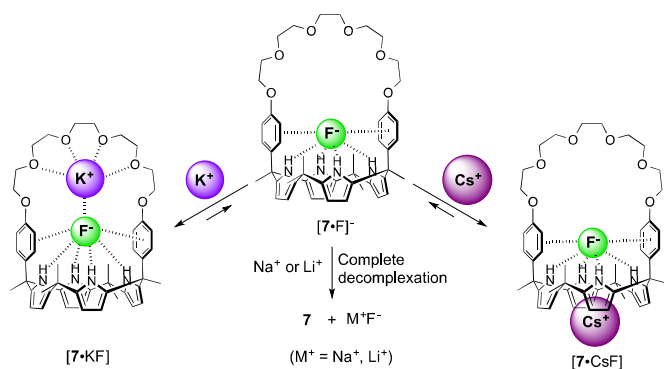


Fig. 9 Effect of treating complex [**7**•F]⁻ (TBA⁺ salt) with perchlorate salts of various alkaline metal cations in 10% CD₃OD/CD₃CN.

In contrast to the previous case, significant downfield shifts were seen in the signals that correspond to oligoether moiety and an upfield shift in the pyrrole NH resonance was seen in the ¹H NMR spectrum (10% CD₃OD/CD₃CN) when [**7**•F]⁻ was treated with KClO₄. Such findings are consistent with the intuitively appealing conclusion that potassium and fluoride form a contact ion pair and are bound within the receptor cavity. With smaller cations, including Li⁺ or Na⁺, complete decomplexation of [**7**•F]⁻ was observed. Presumably, this reflects an attraction between the fluoride anion and lithium or sodium cations that is too strong to be overcome by interaction with the receptor.

The chloride-bound complex of receptor **7** (i.e., [**7**•Cl]⁻; TBA⁺ salt), on the other hand, produces a cavity bound Li⁺Cl⁻ co-complex upon addition of Li⁺ (as the corresponding perchlorate salt) in CD₃CN (Fig. 10). Addition of Cs⁺ (as its perchlorate salt) to [**7**•Cl]⁻ complex in acetonitrile solution gives rise to nearly identical ¹H NMR spectroscopic changes as observed when CsClO₄ is added to the preformed [**7**•F]⁻ complex. A similar binding mode is thus proposed. On the other hand, addition of Na⁺ or K⁺ to [**7**•Cl]⁻ gives rise to a broadening in the ¹H NMR spectral signals. On this basis, it is inferred that these cations serve to induce only partial decomplexation of the initial chloride-bound complex, rather than the complete decomplexation seen in the case of the corresponding fluoride complex, [**7**•F]⁻.

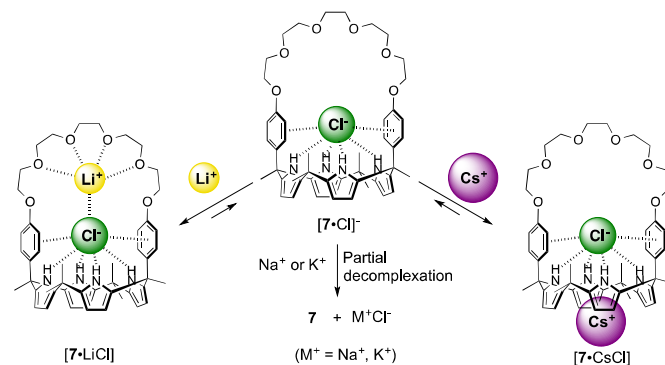


Fig. 10 Cation-induced changes in complexation and decomplexation behaviour observed when complex [**7**•Cl]⁻ is treated with perchlorate salts of various alkaline metal ions in acetonitrile-*d*₃.

The use of **7** as a possible chloride anion carrier was also studied. Toward this end, POPC vesicles were loaded with alkali metal salts, including CsCl, RbCl, KCl and NaCl, and suspended in an external solution containing NaNO₃ or Na₂SO₄ buffered to pH 7.2 using 5 mM sodium phosphate. As shown in Fig. 11, the oligoether-strapped calix[4]pyrrole displays a modest chloride transport ability when the chloride anion counter cation is Na⁺, K⁺ and Rb⁺ and the external phase contains Na₂SO₄. On the other hand, a substantial chloride efflux rate was found when the more lipophilic caesium was used as the counter cation. This increase in transport capability

was ascribed to the participation of a cation/anion co-transport mechanism when the cation was Cs^+ and Na_2SO_4 was present in the external solution.

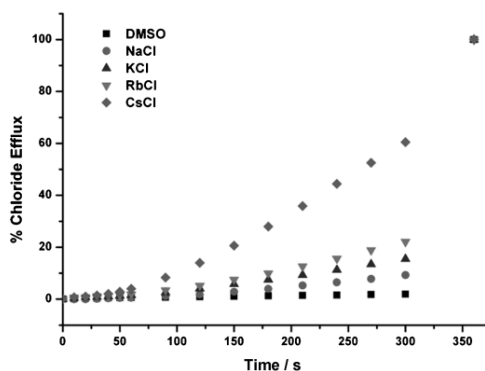


Fig. 11 Chloride efflux promoted by **7** from POPC vesicle loaded with MCl ($M = \text{Na}, \text{K}, \text{Rb}, \text{or Cs}$) in Na_2SO_4 solution. These data provide support for the conclusion that when an anion/cation symport mechanism is not available, chloride efflux from NaCl-containing vesicles can occur *via* a nitrate/chloride antiport process provide the external phase contains the nitrate anion. Copyright 2012 WILEY-VCH Verlag GmbH & Co. KGaA, Weinheim.

Support for the above observation came from so-called U-tube experiments. These experiments involve two aqueous layers – one containing 0.5 M MCl ($M = \text{Cs}^+, \text{K}^+, \text{Na}^+$) in 20 mM phosphate buffer (Aq. 1) and the other consisting of either 0.5 M NaNO_3 or 0.5 M Na_2SO_4 in the same buffered solution (Aq. 2) – that are separated by a dichloromethane layer containing 1 mM of receptor **7**. The transfer of chloride from Aq. 1 to Aq. 2 over 24 h period was monitored at regular intervals using an ion selective electrode. It was found that when Aq. 1 contains either CsCl or KCl, the relative rate of chloride efflux is essentially independent of the choice of salts present in Aq. 2. On the hand, in the case of NaCl, more chloride anion is transferred to Aq. 2 when it contains NaNO_3 rather than Na_2SO_4 . This observation is consistent with the previous vesicle-based results, namely that for the chloride salt of a more hydrophilic cation, Na^+ , an antiport transport mechanism is preferred. Overall, the combination of vesicle and U-tube experiments provides support for the conclusion that the hybrid calix[4]pyrrole **7** is an effective chloride anion transporter, but that the exact mechanism, namely chloride/cation symport *vs.* chloride/nitrate antiport, depends on the choice of cation and conditions.

Nitrate anion transport using calix[4]pyrroles with two electron deficient aromatic walls

Nitrate assimilation is the first key step in biological nitrogen acquisition, which is a pivotal requirement for life.²¹ In many organisms, so-called nitrate transporters (NRTs) actively participate in nitrate uptake. This process provides nitrogen to

animals in organic form, for instance. Nitrate is also of interest because it can act as a chemical signal that regulates carbon metabolism; it does this by modulating the expression of the genes involved in the biosynthesis of organic acids.²² Nevertheless, in spite of the importance of nitrate anion fluxes in living systems, synthetic small molecules capable of acting as nitrate anion transporters are relatively rare.²³

In a recent study, Ballester and coworkers, showed that calix[4]pyrrole derivatives of general structure **8** promoted the selective transport of nitrate over F^- , Cl^- , Br^- , I^- , acetate and perchlorate anions through lipid-based lamellar membranes.²⁴ This study focused on a series of calix[4]pyrrole derivatives bearing two aromatic substituents on opposite *meso* positions (Fig. 12). These substituents act as “walls” whose features could be adjusted to allow the detailed study of anion – π interactions. Toward this end, this team quantified the binding interactions between the nitrate anion and various calix[4]pyrroles **8**. Also studied was octamethylcalix[4]pyrrole **1**. The latter provides a reference value for anion – pyrrole NH hydrogen bonding interactions. By subtracting the value of the H-bonding interaction from values obtained from other calix[4]pyrrole derivatives, the strength of the nitrate – π interaction in question could be deduced. The experimental values were found to correlate linearly with the calculated electrostatic surface potential (ESP) value determined at the centroid of the respective aromatic walls. The strongest anion – π interaction was found in the case of **8e**, as expected.

A single crystal X-ray structure of the nitrate complex $\text{TBA}^+[\mathbf{8e}\cdot\text{NO}_3]^-$ provided support for the lowest energy geometry proposed in solution (Fig. 13). In the solid state structure of **8e**, the nitrate anion is found in an almost orthogonal position relative to the two phenyl rings. The arrangement is as expected for a system wherein the aromatic subunits function as “walls”. The shortest distance between the nitrate oxygen and a carbon atom in the aromatic wall is 3.0 Å. This value is shorter than the sum of the van der Waal radii for each atom. These findings were thus taken as an indication that a degree of weak sigma bonding exists in addition to the proposed anion – π interactions.

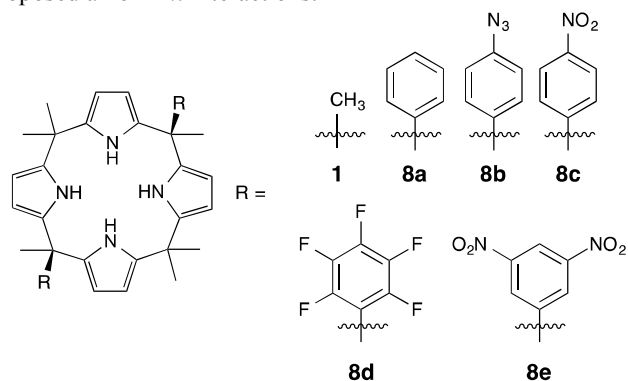


Fig. 12 Molecular structures of the α,α -isomers of the aryl-substituted calix[4]pyrroles **8** and of the parent octamethylcalix[4]pyrrole **1**.

ARTICLE

Table 2. Summary of transport data

| entry | calix-pyrrole | HPTS (NaCl) EC ₅₀ (nM) ^a | HPTS (CsCl) EC ₅₀ (nM) ^a | Cs ⁺ /Na ⁺ ^b | Cl ⁻ /Br ⁻ ^b | NO ₃ ⁻ /Cl ⁻ ^b |
|-------|---------------|--|--|---|---|--|
| 1 | 8a | 350 ± 20 | 9.7 ± 0.4 | 2.8 | 0.9 | 0.8 |
| 2 | 8c | 8.4 ± 3 | 7.3 ± 0.3 | 1.2 | 1.1 | 1.4 |
| 3 | 8e | 2.0 ± 0.4 | 0.73 ± 0.06 | 1.0 | 1.2 | 1.7 |
| 4 | 1 | 960 ± 300 | 4.5 ± 0.3 | Nd | Nd | Nd |

^aEffective calix[4]pyrrole concentration needed to reach 50% activity in the assay. ^bRelative activity in the HPTS assay with different extravesicular ions: External caesium (CsCl) compared with external sodium (NaCl); external chloride (NaCl) compared with external bromide (NaBr); external nitrate (NaNO₃) compared with external chloride (NaCl). HPTS: 8-hydroxy-1,3,6-pyrenetrisulfonate.

The ion transport ability of the calix[4]pyrrole derivatives of general structure **8** was investigated using large unilamellar vesicle (LUVs) made of egg yolk phosphatidylcholine (EYPC) in a HEPES buffered NaCl solution (Table 2). All calix[4]pyrroles derivative **8a-8e** showed chloride transport activity with **8d** and **8e** being the most effective carriers. As in the case of octamethylcalix[4]pyrrole **1**, the double walled calix[4]pyrrole **8a** was found to operate predominantly through a caesium/chloride symport mechanism. On the other hand, **8c** and **8e** transfer chloride mainly *via* an anion/anion antiport mechanism, as inferred from the lack of cation dependence seen in these latter cases (Table 2, Fig. 14).

To obtain a better understanding the relationship between the transport activity and the electronic nature of aromatic walls of calix[4]pyrroles **8** (and presumably, in turn, the interactions of the walls with the anions), an assay was performed under cation-independent conditions. Here, a HEPES buffered NaCl solution was used as the external solution. Under these conditions, a clear relationship between the ESP values of the aromatic walls and the ion transport activity was observed. Most notably, among the calix[4]pyrroles tested, **8c** and **8e** displayed the highest selectivity for nitrate transport (Fig. 14).

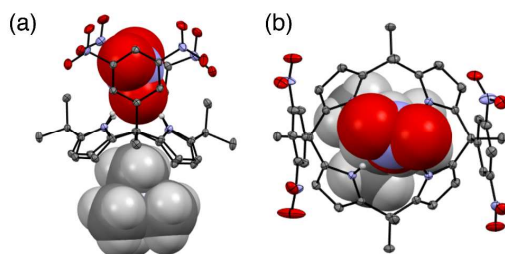


Fig. 13 Side and top view of the binding geometry seen in the solid-state structure of the TMA⁺[**8e**•NO₃⁻] complex. Solvent

molecules and nonpolar hydrogen atoms of **8e** are omitted for clarity. TMA⁺ = tetramethylammonium cation.

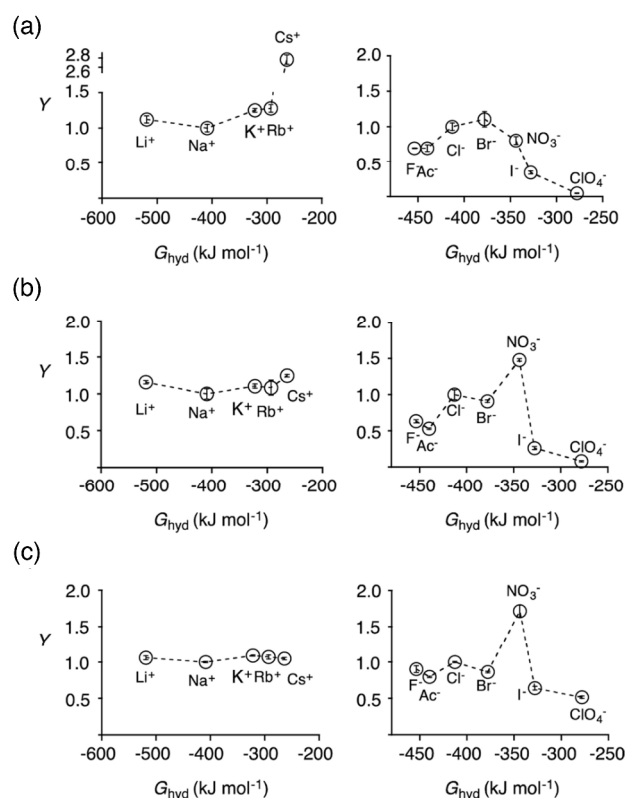


Fig. 14 Transport selectivity. Plots showing the dependence of the fractional transport activity *Y* of calixpyrroles **8a** (a), **8c** (b), and **8e** (c) on the different cations (M^+ as the chloride salts) and anions (as the Na⁺ salts) used in the HPTS ion transport assay. *Y* has been normalized to 1 for Cl⁻ and Na⁺. HPTS: 8-hydroxy-1,3,6-pyrenetrisulfonate. Reprinted with permission from *J. Am. Chem. Soc.*, 2013, **135**, 8324-8330. Copyright 2013 American Chemical Society.

This selective nitrate transport behaviour was attributed to the fact that in these systems the nitrate anion is successfully protected and stabilised by the electron deficient aromatic walls. In conjunction with the hydrogen bonds provided by the calix[4]pyrrole NH protons, this allows for effective recognition and presumably transport, as supported by a X-ray single crystal structure of the nitrate complex of **8e** (Fig. 13).

Calix[4]pyrroles as drug carriers

That calix[4]pyrroles could be used to transport active pharmaceuticals is an appealing notion that, to the authors' knowledge, has so far only been realized successfully in one instance. Specifically, in 2013 Kohnke and co-workers reported the use of a calix[4]pyrrole-*trans*-platinum(II) conjugate as a prodrug, wherein the calix[4]pyrrole plays the role of a drug delivery system.²⁵ To implement this strategy, this research team synthesised the mono *meso*-aminophenyl-functionalised calix[4]pyrrole **9** as a ligand for Pt(II) (Fig. 15). Upon reaction of **9** and *cis*-[PtCl₂(DMSO)₂] in CH₃CN solution, a pale-yellow crystalline product *trans*-Pt-**9** was formed. The progress of the Pt(II) complexation reaction was monitored by ¹H NMR spectroscopy.

Single crystal X-ray diffraction analysis of complex *trans*-Pt-**9** revealed a distorted square planar coordination geometry for the Pt(II) centre with two *trans*-chloride ligands, a finding that provides evidence of configurational isomerisation of the original *cis*-[PtCl₂(DMSO)₂] during the course of the complexation reaction. Overall, the conjugate *trans*-Pt-**9** adopts an U-shaped structure with one DMSO molecule hydrogen-bonded to the calix[4]pyrrole core (Fig. 16).

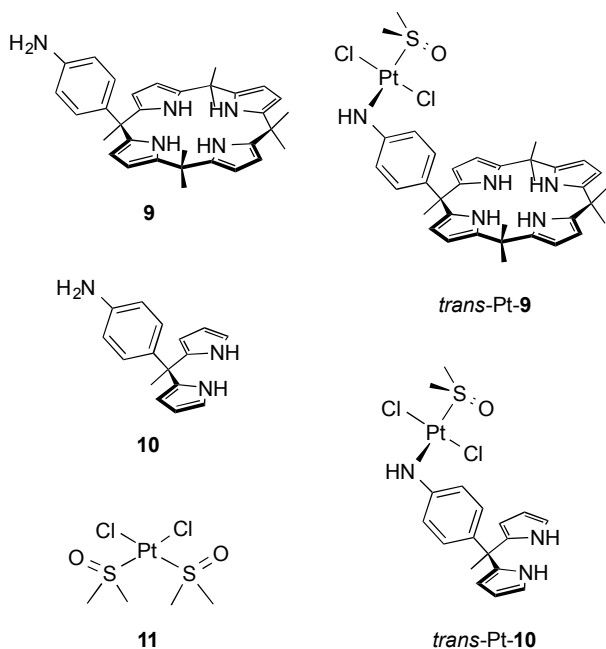


Fig. 15 Molecular structures of **9**, **10** and their Pt conjugates *trans*-Pt-**9** and *trans*-Pt-**10** formed from the reaction of **9** and **10** with the Pt(II) DMSO adduct **11**, respectively.

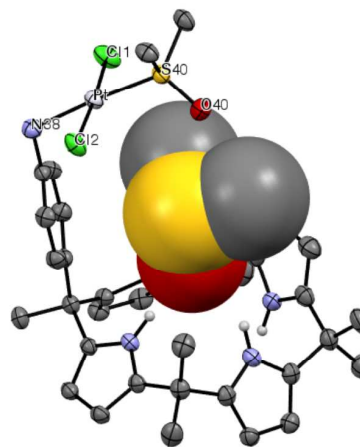


Fig. 16 Single crystal X-ray structure of *trans*-Pt-**9**. Solvent molecules and nonpyrrolic NH hydrogen atoms of **9** are omitted for clarity.

Stability studies of complex *trans*-Pt-**9** carried out in both CD₂Cl₂ and a D₂O/CD₂Cl₂ (20:80, v/v) mixture over 4 h, revealed no appreciable changes in the ¹H NMR spectrum. Even at high concentrations (50 mM) of chloride anion (as the TBA⁺ salt) in D₂O/CD₂Cl₂ (20:80, v/v), only 30% of the Pt(II) was displaced from the conjugate after 24 h.

To investigate the potential utility of *trans*-Pt-**9** to serve as a transport-based prodrug, the ability of the system to transfer Pt(II) to adenosine monophosphate (AMP) was tested. This transfer was followed using ¹H NMR spectroscopy. Upon mixing of *trans*-Pt-**9** and AMP in a 1:1 ratio in CD₃CN at room temperature, the pyrrolic NH signals shift to lower field and become broadened. Such changes are typical of what is observed when an anionic species (phosphate anion of AMP in this case) binds to calix[4]pyrrole through pyrrole N-H...anion hydrogen bond interactions. The actual transfer of the Pt(II) centre to AMP was inferred by the appearance of signals corresponding to **9** and a broadening of the AMP proton resonances. The presence of [Pt(OH)₂(CH₃CN)AMP], [PtCl(OH)(CH₃CN)AMP], [PtCl₂(CH₃CN)AMP], and [PtCl(CH₃CN)(AMP)₂] under conditions of the exchange reaction was also confirmed *via* negative ion mode ESI-MS analyses of a CD₃CN/D₂O solution.

To gain insight into the actual transfer mechanism and the role, if any, the calix[4]pyrrole framework might be playing in the process, the transfer kinetics of Pt(II) were studied in the presence and absence of the calix[4]pyrrole **9**. It was found that the rate of Pt(II) to AMP transfer could be fit well to a first-order model. This is consistent with coordination of the nucleobase taking place within a preformed [*trans*-Pt-**9**•(TBA)₂AMP] complex. The involvement of calix[4]pyrrole-

AMP host-anion interactions was independently supported by a (TBA⁺ salt) was seen to slow the reaction rate. competition experiment, wherein the addition of fluoride anion

Table 3. *In vitro* antiproliferative activity of compounds **9** and **10** and their Pt(II) derivatives, *trans*-Pt-**9** and *trans*-Pt-**10**, compared with that of *trans*- and *cis*-[PtCl₂(NH₃)₂], oxaliplatin, and carboplatin in a human cancer cell-line panel as assessed using an MTT cell viability assay.^a

| compound | A2774 ^b (μ M) | OVCAR3 ^b (μ M) | SKOV3 ^b (μ M) | MDA-MB-231 ^c (μ M) | MCF7 ^c (μ M) |
|---|----------------------------------|-----------------------------------|----------------------------------|---------------------------------------|---------------------------------|
| 10 ^d | >100 ^e | >100 | >100 | >100 | >100 |
| <i>trans</i> -Pt- 10 ^d | 32 \pm 8 | 48 \pm 13 | 46 \pm 16 | 39 \pm 8 | 64 \pm 51 |
| 9 ^d | 98 \pm 60 | 103 \pm 41 | 106 \pm 42 | 89 \pm 12 | 114 \pm 31 |
| <i>trans</i> -Pt- 9 ^d | 23 \pm 3 | 35 \pm 13 | 28 \pm 17 | 26 \pm 12 | 40 \pm 27 |
| <i>trans</i> -[PtCl ₂ (NH ₃) ₂] ^d | >100 | >100 | >100 | >100 | >100 |
| <i>cis</i> -[PtCl ₂ (NH ₃) ₂] ^f | 5 \pm 4 | 6 \pm 2 | 4 \pm 1 | 5 \pm 1 | 18 \pm 12 |
| oxaliplatin ^f | 1.3 \pm 1 | 0.5 \pm 0.1 | 0.7 \pm 0.2 | 1.7 \pm 1 | 1 \pm 0.3 |
| carboplatin ^f | 54 \pm 1 | 56 \pm 2 | 73 \pm 6 | 63 \pm 13 | 89 \pm 7 |

^aValues are IC₅₀, in μ M, expressed as mean values of at least three independent experiments (72 h drug exposure). ^bHuman ovarian cancer cell line. ^cHuman breast cancer cell line. ^dConcentration range from 10 to 100 μ M/L. ^e>100: no activity was detected within the concentration range tested. ^fConcentration range from 0.05 to 500 μ M/L.

A standard MTT (3-[4,5-dimethylthiazol-2-yl]-2,5-diphenyl tetrazolium bromide) cell viability assay involving the A2774, OVCAR-3, and SKOV-3 ovarian carcinoma cell lines also provided evidence that the calix[4]pyrrole skeleton in combination with the coordinated Pt(II) plays a key role in modulating the reactivity of the bound cation. In particular, it was found that both *trans*-Pt-**9** and a dipyrromethane model complex, *trans*-Pt-**10**, have good antiproliferative activity, whereas the corresponding Pt(II) complex not bound to a calix[4]pyrrole core, *trans*-[PtCl₂(NH₃)₂], displays considerably reduced activity. Little or no antiproliferative activity was seen with calix[4]pyrrole **1** or dipyrromethane without a co-complexed or added Pt(II) drug. The results are summarised in Table 3.

Calix[4]pyrrole-based high order aggregates

Spontaneous assembly through molecular recognition is one of the simplest ways to build up complex superstructures that are often difficult to access using conventional covalent bond-forming synthetic strategies.²⁶ The container-like functions of calix[4]pyrroles, namely an ability to recognise and encapsulate various substrates, has made them attractive as building blocks for the creation of new self-assembled structures. Adding to their potential utility in this regard is the fact that 1) the conformation of calix[4]pyrroles may be switched from the normal ground state 1,3-alternate conformation to a inherently less stable cone conformation *via* complexation with an appropriately chosen Lewis basic anion and 2) these two limiting conformations have very different substrate recognitions properties.

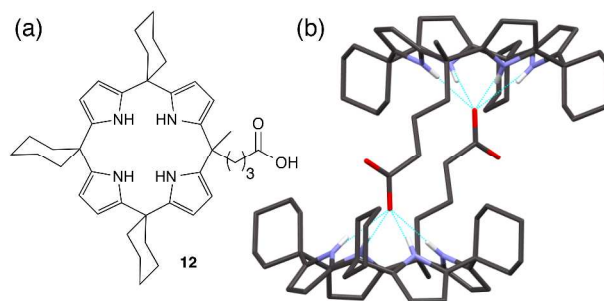


Fig. 17 (a) Chemical structure of compound **12** and (b) the dimeric structure observed in the solid state after deprotonation. Solvent molecules and hydrogen atoms of **12** not involved in the recognition process have been omitted for clarity.

Examples of calix[4]pyrrole self-assembly date back to 1996 when the dimeric structure of the calix[4]pyrrole monoacid **12** was elucidated in the solid state (Fig. 17).²⁷ It was found that this homoditopic complex could be broken up (i.e., disassembled) *via* exposure to a fluoride anion source. While this pointed the way towards the creation of environmentally responsive self-assembled materials, it is only recently that calix[4]pyrroles have been exploited to generate capsule-like systems and stimulus-controlled supramolecular ensembles. One of the first to recognize the broad utility of calix[4]pyrroles in creating self-assembled materials was Ballester. In 2007, his group reported the use of resorcinol-functionalized calix[4]pyrroles **13** to create a hexameric cage of general structure **13**₆ (Fig. 18).²⁸

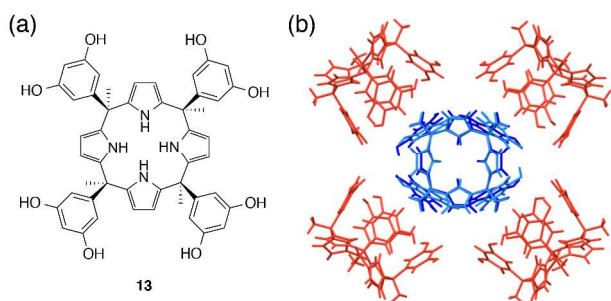


Fig. 18 (a) Chemical structure of resorcinol-functionalized calix[4]pyrrole **13**. (b) Single crystal X-ray structure of hexameric cage **13**₆. Tetramethylammonium cations, chloride anions, and water molecules have been omitted for clarity.

Since then, a number of research papers and reviews have been published by Ballester *et al.*, wherein a range of molecular capsules based on calix[4]pyrroles are described.²⁹⁻³⁵ The Ballester group is also contributing a Tutorial Review entitled “From covalent to supramolecular containers” to this issue of *Chem. Soc. Rev.* Thus, to reduce redundancy we will focus on higher order assemblies (i.e., oligomeric structures) created from calix[4]pyrrole scaffold and their stimulus response features, if any.

In 2004, Nielsen, *et al.* reported a tetrapropyl substituted, tetrathiafulvalene-functionalised calix[4]pyrrole (TTF-C[4]P, **14**, Fig. 19). It was shown that this system, as well as analogues **15** and **16** with extended π -surfaces, could bind neutral, flat, and electron deficient nitroaromatic molecules,^{36,37} including trinitrotoluene (TNT) and trinitrobenzene (TNB), with 1:2 stoichiometry in the absence of coordinating anions in chloroform solution (Fig. 20). In the presence of a coordinating anion, which serves to convert the system to the cone conformation as noted above, no evidence of TNT or TNB binding was observed. The resulting release-of-substrate could be reversed by exposing the chloroform solution containing TTF-C[4]P **14**, the anion salt, and the electron deficient nitroaromatic to water. Subsequently, it was found that the anion bound, cone form of TTF-C[4]Ps **14** and **15** could accommodate larger electron deficient molecules, including C₆₀ and C₇₀ fullerenes as evidenced by both single crystal X-ray diffraction analyses and UV-vis electronic spectral studies.³⁸⁻⁴¹ Recognizing that TTF-C[4]P **14** forms stable complexes with electron deficient nitroaromatics, Sessler and co-workers grafted two dinitrophenyl groups onto the *meso* positions of the basic calix[4]pyrrole core. As prepared, two configurational isomers were obtained, **8e** (reported independently by Ballester²⁴) and **17**.

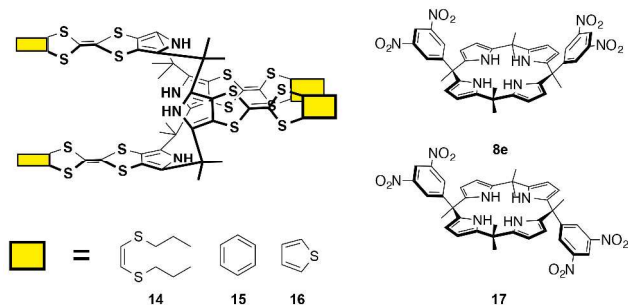


Fig. 19 Chemical structures of tetrathiafulvalene-functionalised calix[4]pyrroles (TTF-C[4]Ps) **14-16** and electron-deficient dinitrophenyl calix[4]pyrroles **8e** and **17**.

With electron rich TTF-C[4]P and *bis*-dinitrophenyl calixpyrroles in hand, Sessler, Bielawski, and collaborators were able to demonstrate in 2011 the formation of chemoresponsive crystalline supramolecular polymeric materials by simple mixing of various combinations of **14-16** with **8e** or **17** in chloroform (Fig. 21).¹² This mixing produces an immediate colour change, from yellow to green. This colour change is correlated with an increase in the spectral intensity around 500 – 800 nm in the absorbance spectrum, which is ascribed to the formation of a charge transfer (CT) complex between the electron-donating TTF units and the electron-accepting dinitrophenyl group. Job plot analyses and 2D ¹H NOESY NMR studies were consistent with a 1:1 binding ratio between the TTF-C[4]P and DNP-C[4]P “monomers”. Isodesmic binding isotherm analyses (CHCl₃) were performed and allowed an effective $K_a = 7.9 \times 10^5 \text{ M}^{-1}$ to be calculated in the case of **16** and **8e** assuming a 1:1 binding mode. This corresponds to an average 20-mer at 1.0 mM, assuming a 1:1 binding mode. Other combinations proved to interact less strongly giving rise to shorter oligomers in chloroform solution. Further evidence for solution phase self-association came from DOSY NMR analyses and light scattering experiments.

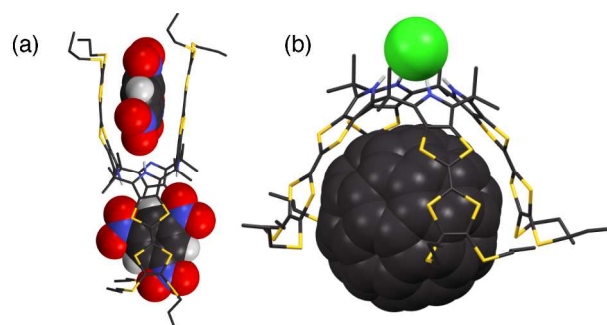


Fig. 20 X-ray single crystal structures of (a) [14•TNB₂] and (b) Li⁺@C₆₀[14•Cl]. Solvent molecules and nonpyrrolic NH hydrogen atoms of **14** are omitted for clarity.

Single crystal X-ray diffraction data revealed that the materials formed from **15** and **17**, as well as **16** and **8e**, exist in the form of one-dimensional polymeric arrays. Based on the structural

parameters, these arrays appear to be stabilised *via* directional hydrogen bond interactions involving the nitro groups of the DNP-C[4]Ps and the pyrrolic NHs from the TTF-C[4]Ps, as well as donor-acceptor interactions between the TTF subunits and the dinitrophenyl groups. Scanning electron microscopic images taken from the polymer dispersion revealed the existence of long and needle-like structures that are consistent with the one-dimensional arrays seen *via* singly crystal X-ray diffraction analysis.

A unique feature of the supramolecular oligomers formed *via* the self-assembly of the TTF-C[4]P and DNP-C[4]P monomers **14-16** and **8e** and **17** is that they are environmentally responsive. For example, addition of TNB to a chloroform solution containing **15** and **17** induces deaggregation of the self-assembled oligomeric materials that exist in the absence of added substrates. Presumably, the free TNB competes with the bulkier and less electron deficient dinitrophenyl functionalised calixpyrrole **17** for the TTF-C[4]P **15**. This competition results in formation of what appears to be a more stable TNB₂⊂TTF-C[4]P complex. This enhanced stability is evidenced by the large increase in the absorption intensity seen in the electronic spectrum upon the addition of TNB to a chloroform mixture of **15** and **17**, as well as the facile isolation of diffraction grade single crystals after allowing the competition reaction to proceed. In solution, an increase in the diffusion constant is also seen, as deduced from DOSY spectral studies.

The addition of a chloride anion source to chloroform solutions of **15** and **17** also leads to deaggregation. Complexation of the chloride anion *via* pyrrolic NH⋯anion hydrogen bonds induces a conformational switch to the cone conformation in the case of both the TTF-C[4]Ps and DNP-C[4]Ps components. Since the electron deficient dinitrophenyl subunits of the DNP-C[4]Ps are not bound well within the deep cavity created by chloride-bound TTF-C[4]Ps, the array undergoes deaggregation. Again, this is reflected in an increase in the diffusion constant.

Single crystals grown from slow diffusion of pentane into a chloroform solution of **15** and **17** under conditions favouring self-assembly containing added tetraethylammonium chloride (TEACl) produced two sets of single crystals consisting of the chloride anion-bound cone conformers of the TTF-C[4]P and DNP-C[4]P “monomers” that give rise to a crystalline, self-assembled aggregate in the absence of TEACl. Of note, is that the relatively small TEA⁺ cation is bound within the calixpyrrole cavity in the case of the TEACl complex of **15**. The net result is an ion pair complex in the solid state (cf. Fig. 21).

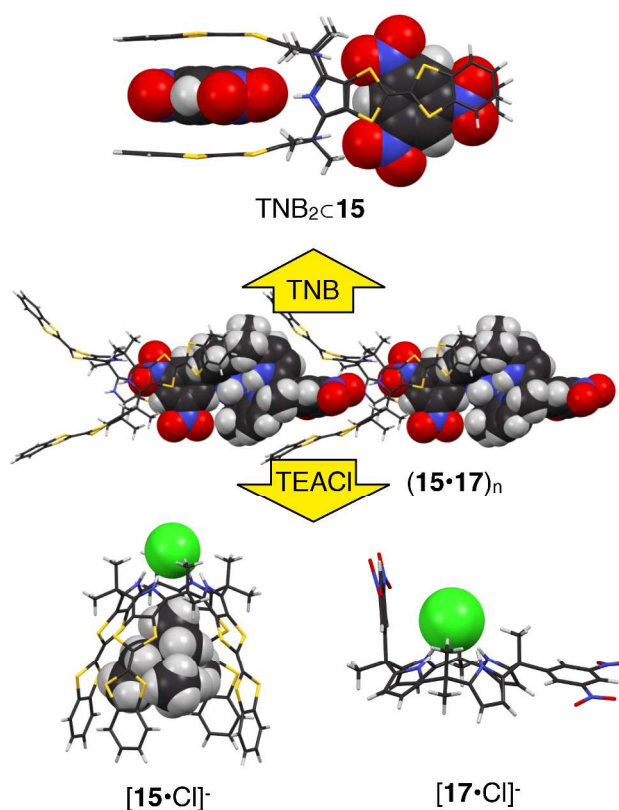


Fig. 21 Single crystal X-ray diffraction structure of the environmentally responsive supramolecular ensemble produced by mixing **15** and **17** in chloroform. Also shown are disassembly processes mediated *via* the addition of trinitrobenzene (TNB) and tetraethylammonium chloride (TEACl), respectively, to chloroform solutions of **15** and **17** and views of the resulting products as determined by single crystal X-ray diffraction analysis.

Sessler and co-workers reported another self-assembled system that was constructed from TTF-C[4]P **15** and an appropriately chosen *trans*-bis(methylpyridinium)-*meso*-substituted calix[4]pyrrole (Pyr-C[4]P) salt, either **18** or **19** (Fig. 22). When the non-coordinating BArF⁻ (tetrakis[bis(3,5-trifluoromethyl)phenyl]borate) anion salt of Pyr-C[4]P (**18**) was used, a linear supramolecular oligomer is formed upon mixing with **15** in a 1:1 ratio in chloroform. This is not true when the corresponding iodide salt (**19**) was used. More generally, the nature of the products formed from mixtures of **15** and **18** or **19** was found to be a tightly coupled function of salts present in solution, as inferred from studies with tetraalkylammonium salts, namely tetraethylammonium BArF⁻ (TEABArF), tetrabutylammonium iodide (TBAI), and tetraethylammonium iodide (TEAI). In fact, mixtures of TTF-C[4]P **15** and Pyr-C[4]P BArF⁻ salt, **18**, give rise to three different supramolecular complexes upon addition of each of these ammonium salts. These consist of a linear polymer, a molecular capsule, and the non-associated monomers, respectively. This system thus provides a rare example wherein well-defined

three-state molecular structures are established from one parent system *via* the simple expedient of modifying the nature (if any) of the external chemical stimulus. In the present instance this modulation came in the form of added organic soluble salts.

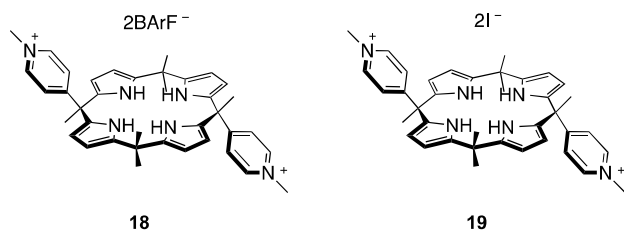


Fig. 22 Chemical structures of the BArF⁻ (**18**) and iodide (**19**) salts of a *trans*-dimethylpyridinium calix[4]pyrrole (Pyr-C[4]P).

The rationale for the stabilisation of three states *via* modulation in the external salt involves the differential binding seen for ostensibly similar anionic and cationic species. The non-coordinating nature of the BArF⁻ anion, means that the addition of the TEA⁺ cation in the form of its BArF⁻ salt (i.e., TEABArF) to a mixture of the TTF-C[4]P **15** and the Pyr-C[4]P **18** in chloroform does not trigger any conformational change in either of the calix[4]pyrrole units. The anion does not bind to the pyrrolic NH protons and does not trigger a conformational change from the 1,3-alternate to cone forms. Therefore, there is no calix[4]pyrrole cavity into which the TEA⁺ cation can be encapsulated. On the other hand, the pyridinium subunits present in the Pyr-C[4]P dication can “intercalate” into the “clefts” that characterize the 1,3-alternate form of the TTF-C[4]P “monomer”. The net result is self-assembly between the electron rich TTF-C[4]P and dicationic Pyr-C[4]P subunits and production of a linear aggregate, (**15•18**)_n, wherein non-coordinating BArF⁻ anions provide for charge balance. This self-associated, oligomeric species is characterized by a maximum at ca. 650 nm in the UV-vis absorption spectrum considered diagnostic of a charge-transfer interaction (cf. Fig 23 top). The solutions also appear green to the eye.

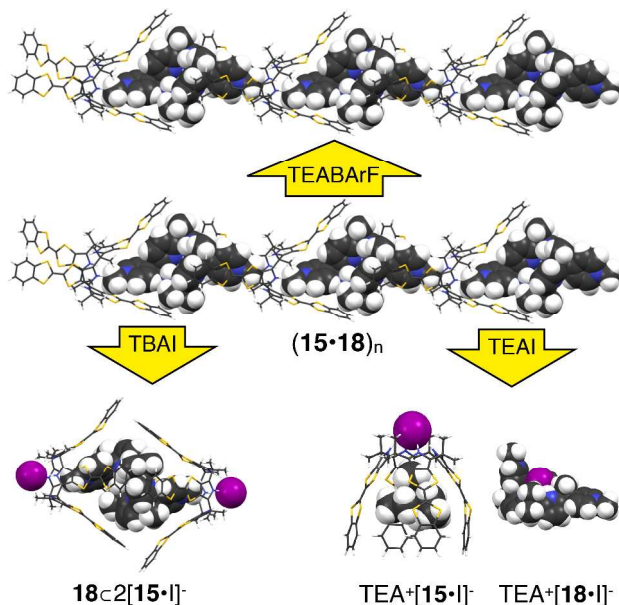


Fig. 23 Schematic representation of the three limiting equilibrium states produced from **15** and **18** *via* treatment with appropriate organic soluble salts. These states are illustrated starting from the self-assembled oligomer, (**15•18**)_n, obtained in chloroform in the absence of any added salt. Changes in this form may be triggered *via* the addition of various tetraalkylammonium salts (2 equiv. each). This allows for formation of a capsule-type species, as well as isolated monomers, as deduced from single crystal structural analyses (Fig. 24). Only the monomeric species are devoid of charge transfer (CT) bands in the UV-vis absorption spectrum. This allows the overall system to function as a NAND logic gate (see main text for details).

When the external salt TEABArF is replaced by TBAI in the above studies, one of the calix[4]pyrroles, namely the electron-rich TTF-C[4]P **15**, undergoes a conformational switch to give its iodide-bound cone conformer. Under the conditions of the experiment the tetrabutylammonium cation is not encapsulated within the bowl-like cavity of the resulting anion complex, [**15•I**]⁻. Rather, the dicationic Pyr-C[4]P **18** is bound in a 2:1 capsule like fashion as shown schematically in Fig. 23. This capsule-like species, wherein a large dicationic calix[4]pyrrole is contained within another neutral calix[4]pyrrole, was characterized both in solution (CHCl₃ and CDCl₃) through a combination of optical and magnetic resonance spectroscopies and in the solid state by means of a single crystal X-ray diffraction analysis (Fig. 24). This capsule structure is stabilised through a combination of supramolecular interactions, including CH \cdots π interactions, ion-pairing interactions, and CT interactions. The latter interactions give rise to the characteristic absorbance maximum at ca. 650 nm and the same green coloured chloroform solutions as seen in the case of the TEABArF-containing mixtures discussed above.

In contrast to what is observed in the case of TBAI, replacement of TEABArF by TEAI serves to break up the self-assembled linear aggregate formed from **15** and **18** into its monomeric constituents. This deaggregation process is driven, presumably, by the formation of a stable ion pair complex, $\text{TEA}^+[\mathbf{15}\cdot\mathbf{I}]^-$, wherein the TEA^+ cation is bound within the bowl-like cavity of $[\mathbf{15}\cdot\mathbf{I}]^-$, as shown schematically in Fig. 23. This species lacks the charge transfer band found for the linear oligomer or the 2:1 capsule-like complex discussed above. Chloroform solutions of this particular mixture are pale orange. The preferential binding of the tetraalkylammonium cation seen in this instance (where the cation is TEA^+), but not in the case of the corresponding studies involving TBAI (where the tetraalkylammonium cation is TBA^+), is ascribed to the relatively smaller size of the TEA^+ cation. Support for this rationale came from single crystal X-ray structural analyses involving both the TEA^+ and the bulkier tetraphenylphosphonium (TPP^+) cations (both studied in the form of their chloride salts). As expected, the smaller TEA^+ cation was found bound within the bowl-like cavity of the $[\mathbf{15}\cdot\text{Cl}]^-$ “container”, whereas the larger TPP^+ cation crystallises in an outside binding mode (cf. Fig. 24). Separate binding isotherm analyses were also carried out. In chloroform solution, it was found that the interaction between TEAI and **15** (effective $K_a = 1.5 \times 10^5 \text{ M}^{-1}$) was slightly greater than that between **15** and **18** (effective $K_a = 1.1 \times 10^5 \text{ M}^{-1}$).

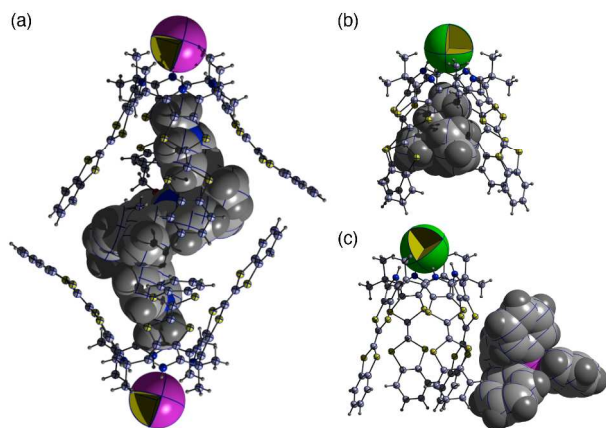


Fig. 24 X-ray single crystal structures of (a) molecular capsule, $\mathbf{15}\cdot\mathbf{19}$, (b) cation-included ion pair complex $\text{TEA}^+[\mathbf{15}\cdot\text{Cl}]^-$, and (c) the cation-excluded congener, $\text{TPP}^+[\mathbf{15}\cdot\text{Cl}]^-$. Adapted with permission from *J. Am. Chem. Soc.*, 2013, **135**, 14889-14894. Copyright 2013 American Chemical Society.

The fact that three separate states may be stabilised from **15** and **18** in the presence of appropriately chosen external salts, allowed the system to be used as a chemical NAND logic device with tetrabutyl- and tetraethylammonium salts being the inputs and the presence (“1”) or absence (“0”) of the charge transfer band being the outputs. As can be seen from an inspection of Fig. 25, only the combination of **15**, **18**, and TEAI

produces an “off” or “0” output; all other mixtures result in systems characterised by an “on” or “1” output.

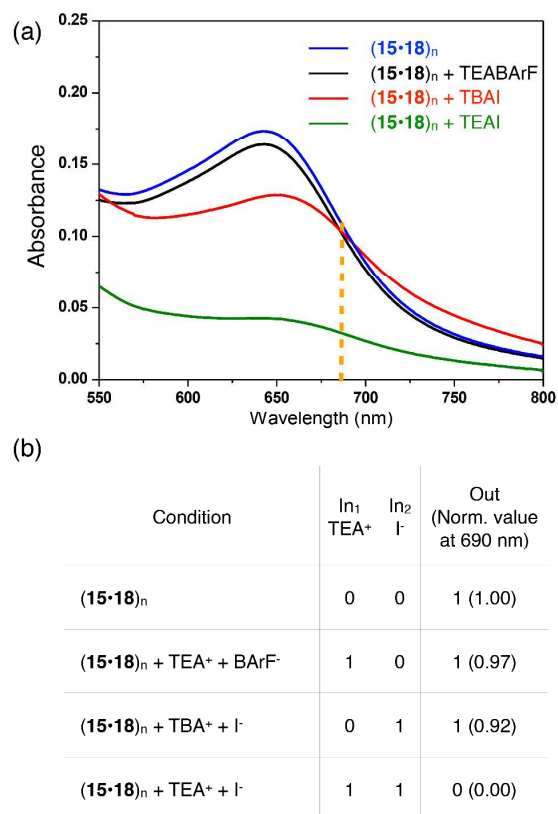


Fig. 25 Logic operations. (a) Charge transfer (CT) response of the self-assembled NAND gate $(\mathbf{15}\cdot\mathbf{18})_n$ seen when the iodide anion (I^-) and the tetraethylammonium (TEA^+) cation are added as inputs. (b) Truth table. Note that both I^- and TEA^+ need to be present in solution (chloroform) in order to produce a “0” output. Adapted with permission from *J. Am. Chem. Soc.*, 2013, **135**, 14889-14894. Copyright 2013 American Chemical Society.

To understand further the determinants that control self-association in calix[4]pyrrole-based systems, the Sessler and Jeppesen groups recently reported the results of a study wherein the rigid dinitrophenyl calix[4]pyrroles **8e** and **17** used by Sessler, Bielawski and collaborators was replaced by a set of flexible *bis*-dinitrophenyl esters (i.e., **20-22**, Fig. 26).¹⁴

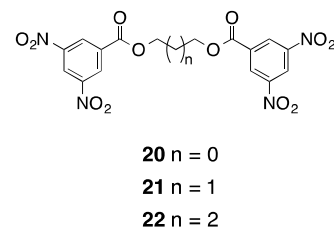


Fig. 26 Chemical structures of the flexible *bis*-dinitrophenyl esters **20-22**

ARTICLE

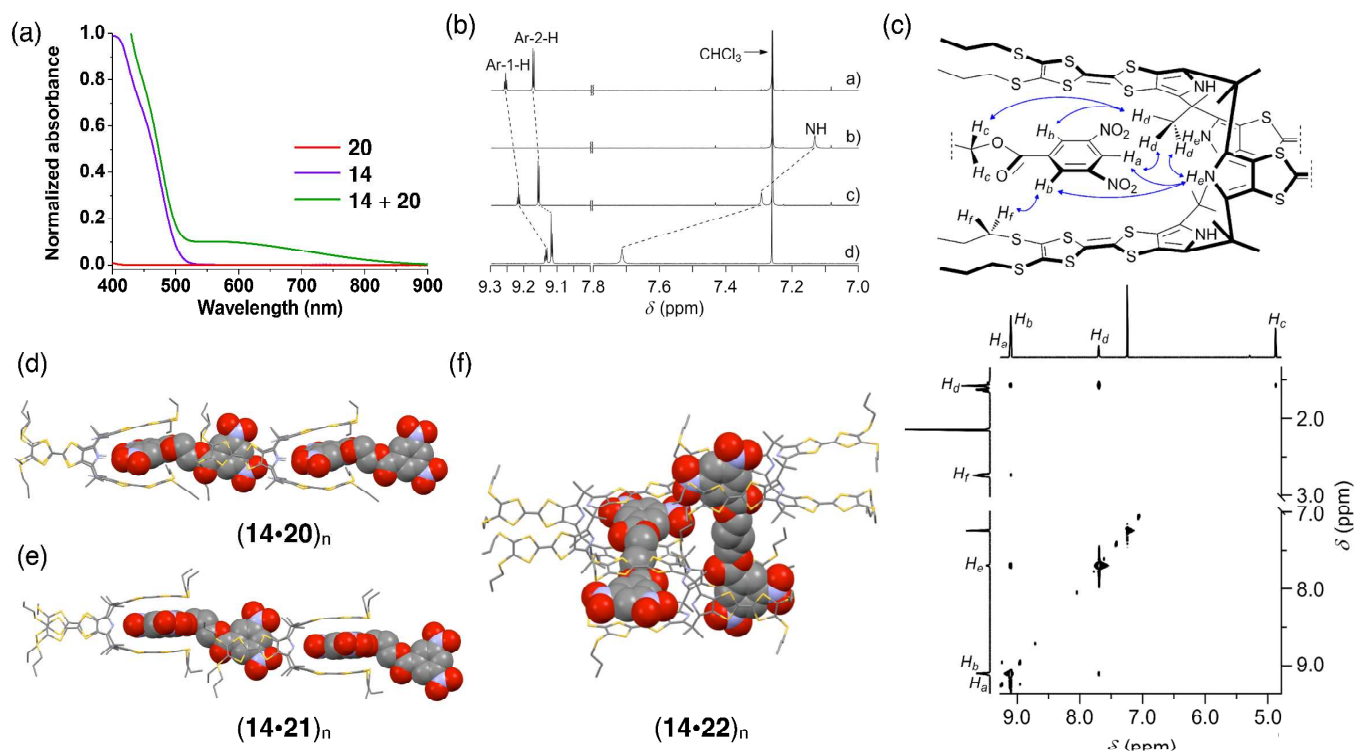


Fig. 27 (a) UV-vis absorption spectra of **14**, **20**, and **14 + 20** as recorded in chloroform at 298 K. (b) Partial ^1H NMR spectra (600 MHz, 298 K) of a) **20** (0.7 mM), b) **14** (0.7 mM), c) **14 + 20** (0.7 mM of **14** and **20**, respectively) and d) **14 + 20** (7.0 mM of **14** and **20**, respectively) all in CDCl_3 . (c) 2D NOESY NMR spectroscopy of **14** (7 mM) and **20** (7 mM) in CDCl_3 . (d-f) X-ray single crystal structures of $(\mathbf{14}\cdot\mathbf{20})_n$, $(\mathbf{14}\cdot\mathbf{21})_n$ and $(\mathbf{14}\cdot\mathbf{22})_n$.

Mixing the thiopropyl functionalised TTF-C[4]P **14** and the bis-dinitrophenyl esters **20-22** in chloroform gave rise to an immediate colour change from yellow to green. This colour change was accompanied by an increase in the absorbance intensity at 566 nm in the UV-vis spectrum. This band, as above, is considered diagnostic of a CT interaction and hence self-association between the species. Evidence for stabilising hydrogen bonding interactions and through-space proton coupling interactions between TTF-C[4]P and the dinitrophenyl moiety of the bis-esters came from 1D and 2D ^1H NMR analyses. Single crystal X-ray diffraction structures, revealing linear, self-assembled solid state polymeric entities, provided further support for the proposal that all three combinations of **14** with **20-22** give rise to self-associated species in chloroform solution (Fig. 27).

Assuming an isodesmic binding model, association constants corresponding to the three supramolecular ensembles in question could be calculated from the concentration-dependent UV-vis spectral changes. The resulting binding constants did not correlate well with linker length. Rather, they were found to reflect the nature of the linker and be dominated by factors, such as steric hindrance within the linker and the dihedral angles of the spacer that connects the two constituent bis-dinitrophenyl moieties present in **20-22** (Fig. 28).

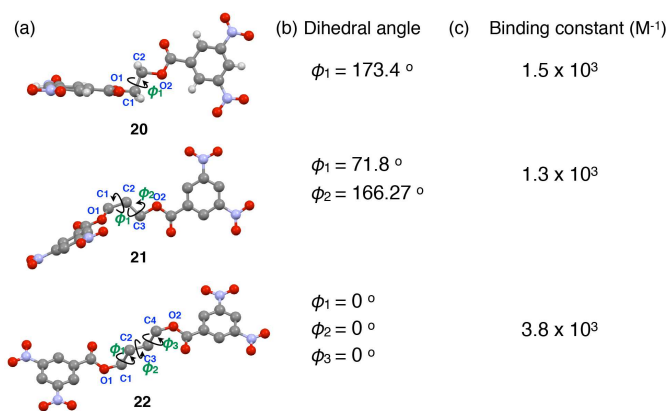


Fig. 28 (a) Single crystal X-ray diffraction structures of **20-22**. (b) Dihedral angles for the linkers present in **20-22** as deduced from the solid state structural parameters. (c) Binding constants calculated from UV-vis spectroscopic titrations carried out in chloroform.

A strong solvent dependence was seen on the aggregation behaviour. This was studied in detail in the case of **14** and **20** using three different solvents, namely 1,2-dichloromethane (DCM), chloroform, and methylcyclohexane (MCH). An inverse relationship between calculated binding constant and solvent polarity was revealed *via* a variable temperature UV-vis spectroscopic study. It was found that in the case of the least polar solvent, MCH, the effective binding constant corresponding to the interaction between **14** and **20** increases by more than two orders of magnitude compared to what was seen in chloroform solution. These differences in association constants are reflected in the degree of polymerization (DPN), with the net aggregate size being substantially larger in MCH than in CHCl₃. They are also reflected in continuous variation analyses (i.e., Job plots), which revealed a slight deviation from clean 1:1 binding in chloroform solution, but not in MCH. This deviation was attributed to the existence of small quantities of less-well-aggregated complexes with net 2:1 stoichiometry.

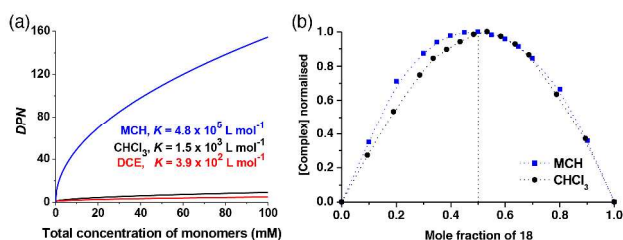


Fig. 29 (a) Plots of degree of polymerization (DPN) as a function of monomer concentration in different solvents, specifically methylcyclohexane (MCH), CHCl₃, and dichloroethane (DCE). (b) Job plots for the solution phase interaction between **14** and **20** as observed in MCH and chloroform, respectively.

Conclusions

Since its first report as an anion binding agent almost two decades ago, calix[4]pyrrole has emerged as a useful receptor system for anions and ion pairs and as a scaffold for further manipulation. Calix[4]pyrroles are attractive systems in that they are easy to functionalise. The original octamethylcalix[4]pyrrole **1** selectively transports CsCl *via* a symport mechanism, whereas replacement of the β -pyrrole protons by fluorine (*via* independent synthesis) changes the transport mechanism from CsCl symport to chloride/nitrate antiport. Modifications of the *meso*-carbon, particularly *via* use of so-called strapping strategies, leads to augmented anion binding affinities and may be used to incorporate additional binding site within the overall framework. These adjustments have been exploited to fine-tune the inherent ion transport modes and have also been used to create a calix[4]pyrrole system that functions as a carrier-based Pt(II) prodrug.

Structural changes from thermodynamically stable 1,3-alternate to cone-like conformations by complexation of anions to the pyrrolic protons serves to alter the selectivity of calix[4]pyrroles towards various analytes, including Lewis basic anions, neutral aromatic molecules (e.g., TNT and TNB), and fullerenes. These switching phenomena have been exploited to create higher order supramolecular self-associated systems that respond to external triggers, including anions, cations, and electron deficient guests. Taking advantage of the selective recognition property of different calix[4]pyrroles, three different limiting molecular structures could be defined, namely monomers, dimers, and oligomers. This has allowed for the creation of a NAND molecular logic device.

Both the use of calix[4]pyrroles as carriers and their use in constructing self-assembled systems involve substrate recognition and encapsulation in some form. Thus, two rapplications serve to highlight the utility of calix[4]pyrroles as container systems capable of recognizing, storing, or transporting guests. In this Review, we have tried to summarize recent progress along these two seemingly disparate tracks so as to illustrate new research directions being pursued with this now-established class of structurally simple receptors.

Acknowledgements

Support for this work came from the Office of Basic Energy Sciences, U.S. Department of Energy (DOE) (grant DE-FG02-01ER15186), the U.S. National Science Foundation (grant CHE-1057904), and the Robert A. Welch Foundation (grant F-1018).

Notes and references

^a Department of Chemistry, The University of Texas at Austin, 105 E. 24th Street, Stop A5300, Austin, Texas 78712-1224, USA.

1. A. Baeyer, *Ber. Dtsch. Chem. Ges.* 1886, **19**, 2184–2185.
2. I.-W. Park, J. Yoo, B. Kim, S. Adhikari, S. K. Kim, Y. Yeon, C. J. E.

- Haynes, J. L. Sutton, C. C. Tong, V. M. Lynch, J. L. Sessler, P. A. Gale, and C.-H. Lee, *Chem. Eur. J.*, 2012, **18**, 2514–2523.
3. D.-W. Yoon, D. E. Gross, V. M. Lynch, C.-H. Lee, P. C. Bennett, and J. L. Sessler, *Chem. Commun.*, 2009, 1109–1111.
 4. J. L. Sessler, D. E. Gross, W.-S. Cho, V. M. Lynch, F. P. Schmidtchen, G. W. Bates, M. E. Light, and P. A. Gale, *J. Am. Chem. Soc.*, 2006, **128**, 12281–12288.
 5. R. Cui, Q. Li, D. E. Gross, X. Meng, B. Li, M. Marquez, R. Yang, J. L. Sessler, and Y. Shao, *J. Am. Chem. Soc.*, 2008, **130**, 14364–14365.
 6. M. Yano, C. C. Tong, M. E. Light, F. P. Schmidtchen, and P. A. Gale, *Org. Biomol. Chem.*, 2010, **8**, 4356–4363.
 7. M. G. Fisher, P. A. Gale, J. R. Hiscock, M. B. Hursthouse, M. E. Light, F. P. Schmidtchen, and C. C. Tong, *Chem. Commun.*, 2009, 3017–3019.
 8. S. J. Moore, M. G. Fisher, M. Yano, C. C. Tong, and P. A. Gale, *Chem. Commun.*, 2011, **47**, 689–691.
 9. C. C. Tong, R. Quesada, J. L. Sessler, and P. A. Gale, *Chem. Commun.*, 2008, 6321–6323.
 10. P. A. Gale, C. C. Tong, C. J. E. Haynes, O. Adeosun, D. E. Gross, E. Karnas, E. M. Sedenberg, R. Quesada, and J. L. Sessler, *J. Am. Chem. Soc.*, 2010, **132**, 3240–3241.
 11. R. Custelcean, L. H. Delmau, B. A. Moyer, J. L. Sessler, W.-S. Cho, D. Gross, G. W. Bates, S. J. Brooks, M. E. Light, and P. A. Gale, *Angew. Chem. Int. Ed. Engl.*, 2005, **44**, 2537–2542.
 12. J. S. Park, K. Y. Yoon, D. S. Kim, V. M. Lynch, C. W. Bielawski, K. P. Johnston, and J. L. Sessler, *Proc. Natl. Acad. Sci. U. S. A.*, 2011, **108**, 20913–20917.
 13. D. S. Kim, V. M. Lynch, J. S. Park, and J. L. Sessler, *J. Am. Chem. Soc.*, 2013, **135**, 14889–14894.
 14. S. Bähring, D. S. Kim, T. Duedal, V. M. Lynch, K. A. Nielsen, J. O. Jeppesen, and J. L. Sessler, *Chem. Commun.*, 2014, **50**, 5497–5499.
 15. C. A. Hübner and T. J. Jentsch, *Hum. Mol. Genet.*, 2002, **11**, 2435–2445.
 16. B. Dworakowska and K. Dołowy, *Acta Biochim. Pol.*, 2000, **47**, 685–703.
 17. Y. Marcus, *Faraday Trans.*, 1991, **87**, 2995–2999.
 18. C.-H. Lee, H.-K. Na, D.-W. Yoon, D.-H. Won, W.-S. Cho, V. M. Lynch, S. V. Shevchuk, and J. L. Sessler, *J. Am. Chem. Soc.*, 2003, **125**, 7301–7306.
 19. D.-W. Yoon, H. Hwang, and C.-H. Lee, *Angew. Chem. Int. Ed. Engl.*, 2002, **41**, 1757–1759.
 20. R. I. S. Diaz, J. Regourd, P. V. Santacroce, J. T. Davis, D. L. Jakeman, and A. Thompson, *Chem. Commun.*, 2007, 2701–2703.
 21. F. Daniel-Vedele, S. Filleur, and M. Caboche, *Curr. Opin. Plant Biol.*, 1998, **1**, 235–239.
 22. W.-R. Scheible, A. González-Fontes, M. Lauerer, B. Müller-Röber, M. Caboche, and M. Stitt, *Plant Cell*, 1997, **9**, 783–798.
 23. P. V. Santacroce, O. A. Okunola, P. Y. Zavalij, and J. T. Davis, *Chem. Commun.*, 2006, 3246–3248.
 24. L. Adriaenssens, C. Estarellas, A. V. Jentsch, M. M. Belmonte, S. Matile, and P. Ballester, *J. Am. Chem. Soc.*, 2013, **135**, 8324–8330.
 25. G. Cafeo, G. Carbotti, A. Cuzzola, M. Fabbi, S. Ferrini, F. H. Kohnke, G. Papanikolaou, M. R. Plutino, C. Rosano, and A. J. P. White, *J. Am. Chem. Soc.*, 2013, **135**, 2544–2551.
 26. D. Philp and J. F. Stoddart, *Angew. Chem. Int. Ed. Engl.*, 1996, **35**, 1154–1196.
 27. J. L. Sessler, A. Andrievsky, P. A. Gale, and V. Lynch, *Angew. Chem. Int. Ed. Engl.*, 1996, **35**, 2782–2785.
 28. G. Gil-Ramírez, J. Benet-Buchholz, E. C. Escudero-Adán, and P. Ballester, *J. Am. Chem. Soc.*, 2007, **129**, 3820–3821.
 29. P. Ballester and G. Gil-Ramírez, *Proc. Natl. Acad. Sci. U. S. A.*, 2009, **106**, 10455–10459.
 30. G. Gil-Ramírez, M. Chas, and P. Ballester, *J. Am. Chem. Soc.*, 2010, **132**, 2520–2521.
 31. M. Chas and P. Ballester, *Chem. Sci.*, 2012, **3**, 186–191.
 32. B. Verdejo, F. Rodríguez-Llansola, B. Escuder, J. F. Miravet, and P. Ballester, *Chem. Commun.*, 2011, **47**, 2017–2019.
 33. M. Chas, G. Gil-Ramírez, and P. Ballester, *Org. Lett.*, 2011, **13**, 3402–3405.
 34. P. Ballester, *Isr. J. Chem.*, 2011, **51**, 710–724.
 35. L. Adriaenssens and P. Ballester, *Chem. Soc. Rev.*, 2013, **42**, 3261–3277.
 36. K. A. Nielsen, W.-S. Cho, J. O. Jeppesen, V. M. Lynch, J. Becher, and J. L. Sessler, *J. Am. Chem. Soc.*, 2004, **126**, 16296–16297.
 37. J. S. Park, F. Le Derf, C. M. Bejger, V. M. Lynch, J. L. Sessler, K. A. Nielsen, C. Johnsen, and J. O. Jeppesen, *Chem. Eur. J.*, 2010, **16**, 848–854.
 38. K. A. Nielsen, W.-S. Cho, G. H. Sarova, B. M. Petersen, A. D. Bond, J. Becher, F. Jensen, D. M. Guldi, J. L. Sessler, and J. O. Jeppesen, *Angew. Chem. Int. Ed. Engl.*, 2006, **45**, 6848–6853.
 39. K. A. Nielsen, G. H. Sarova, L. Martín-Gomis, F. Fernández-Lázaro, P. C. Stein, L. Sanguinet, E. Levillain, J. L. Sessler, D. M. Guldi, Á. Sastre-Santos, and J. O. Jeppesen, *J. Am. Chem. Soc.*, 2008, **130**, 460–462.
 40. S. Fukuzumi, K. Ohkubo, Y. Kawashima, D. S. Kim, J. S. Park, A. Jana, V. M. Lynch, D. Kim, and J. L. Sessler, *J. Am. Chem. Soc.*, 2011, **133**, 15938–15941.
 41. C. M. Davis, J. M. Kim, K. R. Larsen, D. S. Kim, Y. M. Sung, D. M. Lyons, V. M. Lynch, K. A. Nielsen, J. O. Jeppesen, D. Kim, J. S. Park, and J. L. Sessler, *submitted*.

TOC Graphic and one-sentence summary.

Calix[4]pyrroles function as “molecular containers” as illustrated by their ability to act as carriers for the through-membrane transport of ions and as “monomers” in the construction of aggregated supramolecular constructs.

